FUEL CYCLE AND WASTE MANAGEMENT

Sponsored by the Fuel Cycle and Waste Management Division

Cosponsored by the Nuclear Criticality Safety Division

1. An Empirical Approach to Bounding the Axial Reactivity Effects of PWR Spent Nuclear Fuel, *Patrick M. O'Leary (Framatome, Lynchburg), John M. Scaglione (Bechtel SAIC)*

INTRODUCTION

One of the significant issues yet to be resolved for using burnup credit (BUC) for spent nuclear fuel (SNF) is establishing a set of depletion parameters that produce an adequately conservative representation of the fuel's isotopic inventory. Depletion parameters (such as local power, fuel temperature, moderator temperature, burnable poison rod history, and soluble boron concentration) affect the isotopic inventory of fuel that is depleted in a pressurized water reactor (PWR). However, obtaining the detailed operating histories needed to model all PWR fuel assemblies to which BUC would be applied is an onerous and costly task. Simplifications therefore have been suggested that could lead to using "bounding" depletion parameters that could be broadly applied to different fuel assemblies. This paper presents a method for determining a set of bounding depletion parameters for use in criticality analyses for SNF.

DESCRIPTION

The general method for determining a set of bounding depletion parameters can be accomplished in six steps. Step one involves identifying the fuel type to which the BUC will be applied. In step two, a statistically significant number of representative fuel-depletion operating histories are surveyed. Information about burnup, fuel temperature, soluble boron, moderator density, burnable poison use, and control-rod insertion history are collected for each fuel assembly. Step three analyzes the survey results to determine the range of expected values, including a mean and standard deviation (where applicable). Step four identifies the bounding values for each depletion parameter, and step five uses these depletion parameters as input to an isotopic depletion computer code such as SAS2H (Ref. 1) or CASMO-3 (Ref. 2) to determine the discharge isotopic inventory. Finally, step six uses this isotopic inventory in a waste package MCNP (Ref. 3) computer model to determine the k_{eff} for a sample loading of SNF. A parallel set of isotopics is determined from a depletion calculation based on actual depletion history conditions for selected assemblies. The results from these calculations are compared to demonstrate that the reactivity of the SNF in a waste package using the bounding model is always greater than the waste package reactivity calculation using the actual depletion history isotopic inventory.

RESULTS

The operating histories from approximately 3400 individual PWR fuel assemblies were surveyed to demonstrate this method. Fuel-cycle boron letdown curves, average fuel power densities, burnable poison history, control rod history, and moderator temperature data were collected for individual fuel assemblies from a total of seven different reactors designed by either Babcock & Wilcox (B&W) or Westinghouse. The survey provides an "expected range of values" for each depletion parameter as a function of axial position. A fuel model was depleted using a bounding maximum or minimum value for each parameter. The nature of the bounding value was determined by its tendency to increase reactivity, generally as a result of neutron spectrum hardening. The sensitivity on k_{eff} was evaluated for two different assemblies according to the conditions described in Table I. Assembly F6 is a 15×15 B&W assembly with an initial enrichment of 3.49 wt% ^{235}U. This assembly used burnable poison rods (BPRs) for one cycle, and it was depleted to an average burnup

TABLE I

Summary of Bounding Depletion Parameters

Case	Depletion Parameters				
	Assembly Burnup	Fuel Temperature	Moderator Density	Soluble Boron	Burnable Poison Rod History
1	Actual	Actual	Actual	Actual	Actual
2	Minimum	Maximum	Minimum	Maximum	Inserted 1'st cycle
3	Minimum	Maximum	Minimum	Maximum	None
4	Minimum	Actual	Actual	Actual	Actual
5	Minimum	Actual	Actual	Actual	None
6	Actual	Maximum	Actual	Actual	Actual
7	Actual	Actual	Minimum	Actual	Actual

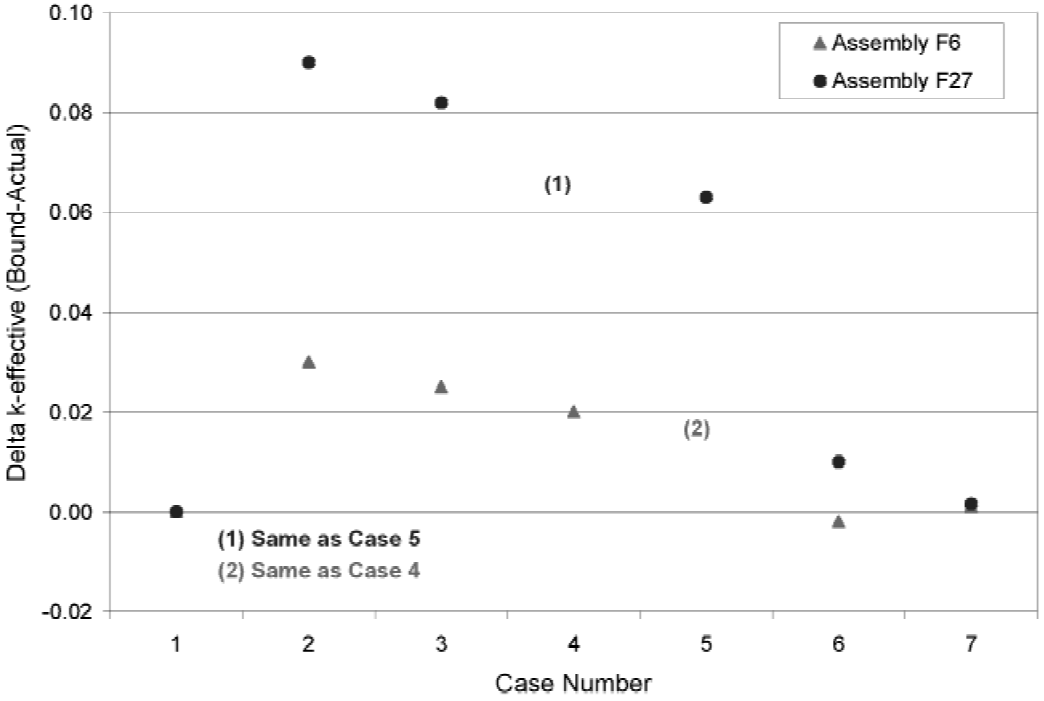

Fig. 1. Summary of depletion parameter sensitivity evaluations.

of 16.8 GWd/tonne U. Assembly F27 is also a 15 × 15 B&W assembly with an initial enrichment of 3.49 wt% ^{235}U. This assembly had no BPRs, and it was depleted to an average burnup of 33.6 GWd/tonne U. Figure 1 presents the results of the sensitivity calculations, which show a wide variation in conservatism relative to the actual depletion conditions. Case 1 represents the base case (actual) for each assembly. Case 2 results indicate that using bounding values for all of the depletion parameters produces very conservative results, perhaps too much so. The other cases show sensitivities for each depletion parameter selected.

This study demonstrates that operating-history information provides a realistic basis for establishing "bounding" values. Many different models can be developed to conservatively bound the expected reactivity of PWR SNF. End-user design/licensing criteria will determine the most appropriate for their needs.

1. SAS2H-SCALE: "A Modular Code System for Performing Standardized Analyses for Licensing Evaluations," NUREG/CR-0200, Rev. 4 (ORNL/NUREG/CSD-2/R4) (Apr. 1995).

2. "CASMO-3, A Fuel Assembly Burnup Program, Version 4.8," Studsvik/NFA-89/3 (Nov. 1996).

3. "MCNP—A General Monte Carlo N-Particle Transport Code," LA-12625-M, Version 4B, J. F. BRIESMEISTER, Ed., Los Alamos National Lab. (1997).

2. Design of a BWR Core with Overmoderated MOX Fuel Assemblies, *J. L. François, C. Martín del Campo (UNAM–Mexico)*

INTRODUCTION

The use of uranium-plutonium mixed-oxide (MOX) fuel in light water reactors is a current practice in several countries. Generally one-third of the reactor core is loaded with MOX fuel assemblies, and the other two-thirds is loaded with uranium assemblies. Nevertheless, the plutonium utilization could be more effective if the full core could be loaded with MOX fuel. In this work, the design of a boiling water reactor (BWR) core fully loaded with overmoderated MOX fuel designs was investigated.

In previous work,[1] the design of overmoderated BWR MOX fuel assemblies based on a 10 × 10 lattice was presented; these designs improve the neutron spectrum and the plutonium consumption rate, compared with standard MOX assemblies. To increase the moderator-to-fuel ratio (MFR), two approaches were followed. In the first approach, 8 or 12 fuel rods were replaced by water rods in the 10 × 10 assembly, which increased the MFR from 1.9 to 2.2 and 2.4, respectively. These designs are called MOX-8WR and MOX-12WR, respectively, in this paper. In the second approach, an 11 × 11 lattice with 24 water rods (11 × 11-24WR) was designed, which is a design with a number of active fuel rods (88) very close to the standard MOX assembly (91). The fuel rod diameter is smaller to preserve the assembly dimensions, and in this last case, the MFR is 2.4.

METHODOLOGY

The calculations were performed with the CM-PRESTO three-dimensional steady-state simulator.[2] The nuclear data banks were generated with the HELIOS system,[3] and they were processed by TABGEN to produce tables of nuclear cross sections depending on burnup, void, and exposure weighted void (void history), which are used by CM-PRESTO. One base reload pattern was designed for a BWR/5 rated at 1931 MW(thermal), to be used with the different overmoderated assembly designs. The reload pattern has 112 fresh fuel assemblies (FFAs) out of a total of 444 fuel assemblies and was simulated during 20 cycles with the Haling strategy, until an equilibrium cycle of 365 effective full-power days (EFPDs) was obtained.

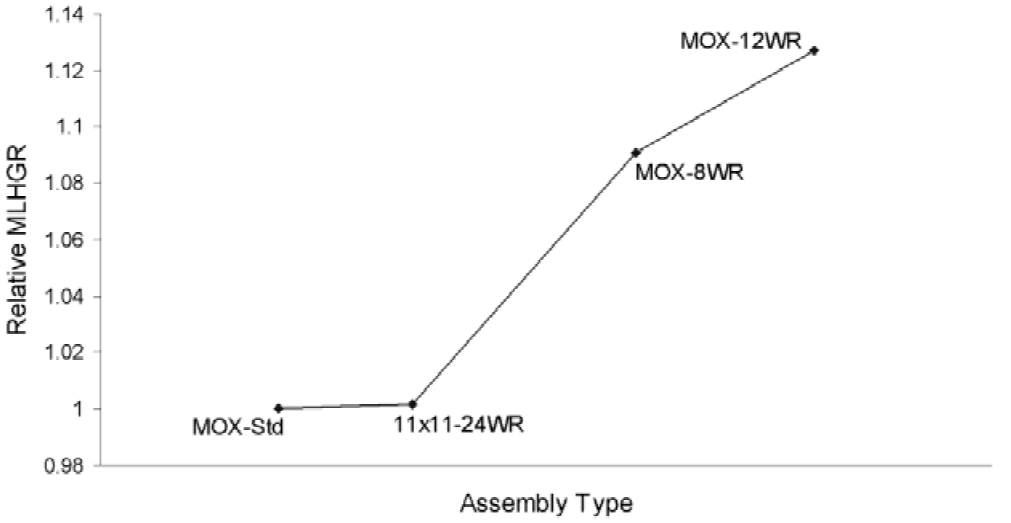

Fig. 1. Maximum lineal heat generation rate behavior relative to the assembly type in the core.

RESULTS

Table I shows the main results for different configurations of overmoderated fuel assemblies and for the standard MOX fuel assembly. The results show that the cases with the overmoderated assemblies do not obtain the 365-EFPD cycle length because the heavy-metal inventory of the core with overmoderated assemblies is smaller than the core with standard MOX assemblies since the overmoderated assemblies have fewer fuel rods. To obtain the desired cycle length, a reload of 128 FFAs was designed for the case with the 11×11 fuel assembly type and a reload of 120 FFAs for the case of 12 water rods in the 10×10 lattice. For this last assembly type, the cycle length obtained with a reload of 128 FFAs is higher than the cycle length obtained with the 11×11 fuel assembly because the plutonium fissile average enrichment is higher in the 10×10 assembly with 12 water rods, as can be seen in Table I. Regarding the relative power values, they are close in all the cases and quite standard for Haling calculations. Figure 1 shows the behavior of the core relative maximum lineal heat generation rate (MLHGR) for different assembly types; it can be seen that the MLHGR of the 11×11 assembly is very close to that of the standard MOX assembly.

CONCLUSIONS

An 11×11 design was proposed with an active fuel length very close to the standard MOX assembly. It has been shown that for a full core loaded with overmoderated MOX assemblies, this design takes advantage of the softer spectrum comparable to the 10×10 lattice with 12 water rods but with thermal limits (MLHGR) comparable to the standard MOX fuel assembly.

1. J. L. FRANÇOIS, J. HERNANDEZ, "A Study of the Overmoderated BWR-MOX Fuel Assembly," *Trans. Am. Nucl. Soc.*, **83**, 45 (2000).

2. "User Manual CM-PRESTO-91," Scandpower (1993).

3. J. J. CASAL, R. J. J. STAMM'LER, E. A. VILLARINO, A. A. FERRI, "HELIOS: Geometric Capabilities of a New Fuel Assembly Program," *Proc. Int. Topl. Mtg. Advances Mathematics, Computations and Reactor Physics*, Pittsburgh, Pennsylvania, 1991, Vol. 2, p. 10.2.1 1-13 (1991).

TABLE I
Equilibrium Cycle Simulation Main Results

Case	Cycle Length (EFPD)	Core Heavy Metal Weight (tonnes)	Radial Power Peaking Factor	Max. Relative Nodal Power	Max. Assembly Burn-up (MWd/MT)	Assembly Avg. Enr. Pu Fiss (%)
MOX Std. (**112 FFA**)	**367.3**	**82.4**	1.416	1.805	37 590	**3.92**
11×11-24WR (112 FFA)	333	71.9	1.423	1.748	38 820	3.32
11×11-24WR (**128 FFA**)	**366.2**	**71.9**	1.412	1.770	41 150	**3.32**
MOX-8WR (112 FFA)	314.7	75.2	1.415	1.796	35 210	3.36
MOX-8WR (128 FFA)	345.3	75.2	1.395	1.812	37 200	3.36
MOX-12WR (112 FFA)	345.8	71.5	1.417	1.766	40 570	3.62
MOX-12WR (**120 FFA**)	**360.6**	**71.5**	1.391	1.746	41 720	**3.62**
MOX-12WR (128 FFA)	380.4	71.5	1.404	1.785	42 950	3.62

3. Analysis of PWR Equilibrium Fuel Cycles Using Nuclide Importance, *Hiroshi Sekimoto, Abdul Waris (Tokyo Inst Technol–Japan)*

Energy generation by nuclear reactors entails production of plutonium and radioactive waste. To utilize the plutonium and to minimize the long-term radiotoxic waste, an option is a closed fuel cycle strategy employing reprocessing and recycling of actinides. Since commercial operation of fast reactors is not considered to be realized in the near future, plutonium and minor actinide recycling in light water reactors (LWRs) is considered, although LWR neutron economy is not good.

In this study, uranium enrichment, natural uranium requirements, and toxicity of discharged heavy metals (HMs) are evaluated for a pressurized water reactor (PWR), whose design parameters are given in Table I. The following fuel cycles are investigated, where all fission products (FPs) and final products of HMs (Tl-Fr) are discharged from the reactor at a standard rate (25%/yr):

Case 1: All HMs are discharged with the standard rate.

Case 2: All HMs except Pu are discharged with the standard rate; Pu is discharged at the rate of one-half of the standard rate.

Case 3: All HMs except Pu are discharged with the standard rate; Pu is confined.

Case 4: All HMs except U are confined; U is discharged with the standard rate.

Case 5: All HMs are confined.

The infinite multiplication factor k can be expressed by using the nuclide importances (fission neutron importance f_j and absorbed neutron importance a_j) as

$$k = \frac{\sum_j f_j s_j}{\alpha \sum_j a_j s_j} ,$$

where

s_j = atomic percent of uranium isotopes (^{234}U, ^{235}U, and ^{238}U) in the supplied fuel

α = correction factor for estimating neutron absorption by non-fuel-originating nuclides, such as coolant and construction materials.

A detailed description of nuclide importance and calculation method is given in Ref. 1. The value k is set to be 1.02, and s_j are evaluated from this equation and the following ones:

TABLE I

Design Parameters of Studied PWR

Power output [MW(thermal)]	3000
Average power density (W/cm^3)	
In pellet	280
In cell	100
Fuel pellet diameter (mm)	8
Pin diameter (mm)	9.6
Pin pitch (mm)	11.8
Materials	
Fuel pellet	Oxide
Cladding	Zircaloy 4
Coolant	Light water

$$s_{24} + s_{25} + s_{28} = 100$$

and

$$100 s_{24} - 0.9937 s_{25} = -0.1925 .$$

The second equation is given by enrichment conditions. The group cross-section set is generated with the SRAC code system[2] using the JENDLE-3.2 library.[3]

Table II shows some of calculation results from this study. The importance changes in different ways between ^{235}U and ^{238}U, and changes for ^{235}U are larger. However, since the s_j of ^{238}U is much larger than ^{235}U, effects of ^{238}U are dominant. The enrichment as well as the required amount of natural uranium decreases considerably with increasing number of confined heavy nuclides when uranium is discharged from the reactor. The burnup changes inversely proportional to the amount of charged fuel.

Figure 1 (see next page) shows the change of toxicity ratio of discharged HMs to that of fed fuel a long time after discharge of fuel from the reactor. The value for case 5 is zero and is not shown. For case 4, the toxicity of discharged fuel becomes slightly smaller than one of charged uranium.

1. H. SEKIMOTO, A. NEMOTO, "Nuclide Importance and the Steady-State Burnup Equation," *Nucl. Sci. Eng.*, **135**, 84 (2000).

2. K. OKUMURA et al., "SRAC95; General Purpose Neutron Code System," JAERI-Data/Code-96-015, Japan Atomic Energy Research Institute (1996).

TABLE II

Calculated Nuclide Importances and Fuel Cycle Characteristics

Case	α	^{235}U		^{238}U		Enrichment (%)	Charge rate (t/yr)	Burnup (GWd/t)	Required natural U	
		f	a	f	a				0.1% tail (t/yr)	0.3% tail (t/yr)
1	1.03	1.07	0.69	0.07	0.08	5.4	22	49.9	190.1	271.9
2	1.02	1.00	0.64	0.07	0.08	5.2	21.8	50.3	181.7	259.6
3	1.01	0.83	0.54	0.09	0.09	4.9	21.2	51.6	167.2	238.2
4	1.01	0.79	0.54	0.09	0.10	4.8	20.8	52.7	158.4	225.4
5	1.01	2.56	2.23	2.93	3.05	44.7	1.2	937.3	85.4	126.4

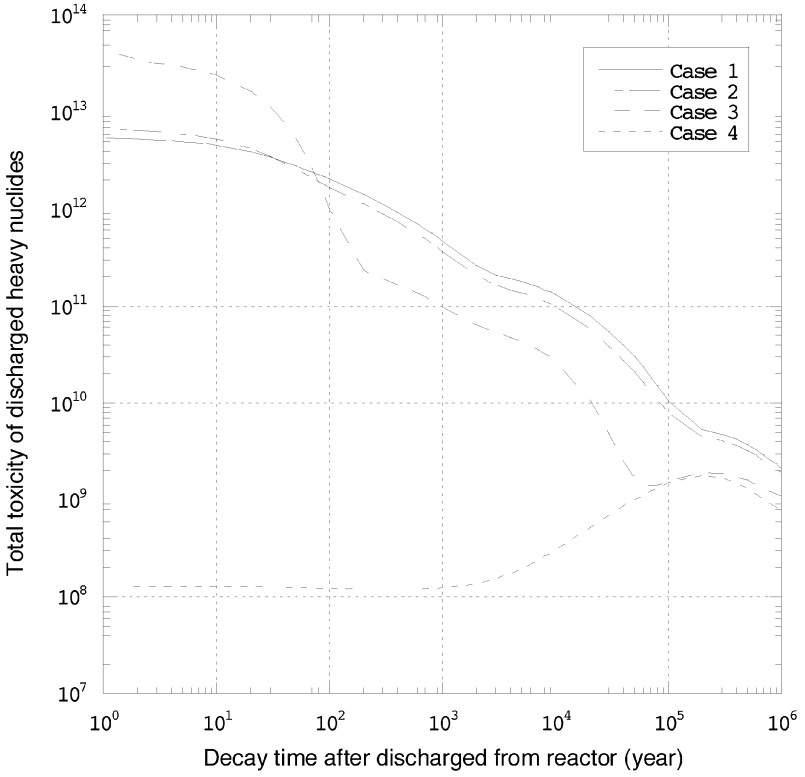

Fig. 1. Toxicity ratio of discharged HMs to fed fuel. (Paper 3)

3. T. NAKAGAWA et al., "Japanese Evaluated Nuclear Data Library Version 3 Revison-2: JENDL-3.2," *J. Nucl. Sci. Technol.*, **32**, 1259 (1996).

4. Using the Water Displacer Rod Concept to Improve the Fuel Utilization of SMART, *Yong Se Kwon, Un Chul Lee (Seoul Natl Univ–Korea)*

INTRODUCTION

In this study, the water displacer rod (WDR) concept based on spectral shift technology was introduced to increase the fuel utilization of the System-integrated Modular Advanced ReacTor (SMART) while minimizing the core design changes and the effects on the core safety. The WDR concept is a kind of mechanical spectral shift technology.

SMART is a nuclear reactor of small capacity, 330 MW(thermal), and it has been developed by the Korea Atomic Energy Research Institute for the purpose of local heating and disalination of seawater. The refueling cycle and the fuel enrichment of SMART are 36 months and 4.95 wt%, respectively. The single-batch core is adapted for the convenience of maintenance activity. Especially, the core of SMART is a soluble boron free core.

DESCRIPTION OF THE ACTUAL WORK

To predict the effect of WDR on the fuel utilization of SMART, a sensitivity analysis of the point of time and the numbers of WDR insertion/withdrawal was performed. The change of k_∞ and the mass fraction of the residual fissile material were evaluated in the case of WDR application. To maximize the effect of WDR, the core was rearranged according to the sensitivity analysis. Figures 1a and 1b show the change of k_∞ and the mass fraction of the fissile material for burnup increment.

Burnup calculations were performed for the SMART cores with and without WDR. To evaluate the effect of WDR, the critical control rod positions for the burnup increment were compared for the two cases. Figure 2a shows the results of the comparison. WDR insertion is performed at 0 and 200 effective full-power days (EFPDs). WDR withdrawal is performed at 50 and 900 EFPDs.

To evaluate the effect of WDR on the core safety, the three-dimensional local power peaking factor (F_q) and cold shutdown reactivity were analyzed. The maximum F_q of the core with WDR was 2.7154, and the cold shutdown reactivity was 0.98614. For each burnup step, the axial offsets of each case were analyzed, and Fig. 2b shows the result.

RESULTS

According to the results of the burnup analysis, the cycle length increment is ~5 EFPDs. The cycle length did not increase as expected because of two following reasons. First, because of the high residual fuel enrichment, the effect of fissile plutonium was not remarkable. Second, the neutron absorption by burnable poison overwhelms that by fertile uranium. Therefore, conversion of fertile material to fissile material did not occur as much as expected.

According to the results of the safety analysis, WDR application did not harm the reactor safety.

In terms of the fine reactivity control capability of the WDR concept, it is worthy of application to the field of fuel management through the further studies on the optimization for the enrichment of the fuel and burnable poison.

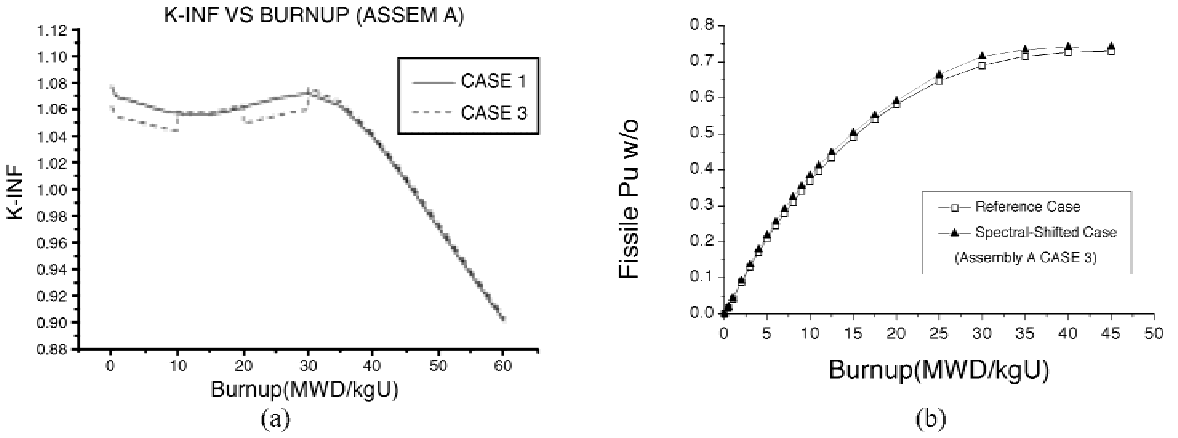

Fig. 1. The result of sensitivity analysis. (Paper 4)

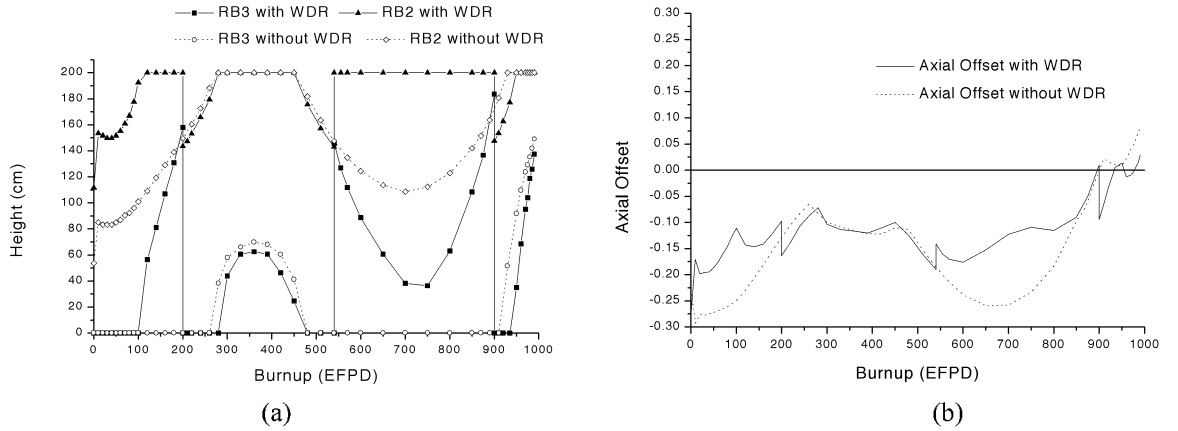

Fig. 2. The result of reactor core analysis. (Paper 4)

5. Validation of Argonne National Laboratory Dose Calculations for BN-350 Spent Fuel, *R. W. Schaefer (ANL-Idaho)*

Gamma-ray (gamma) dose calculations are being made in support of the joint U. S. Department of Energy/Kazakhstan disposition project for spent fuel from the BN-350 fast breeder reactor. The calculations are used to predict the self-protection status of individual fuel assemblies and loaded storage canisters, as well as to design shields. Accordingly, it is important to validate these calculations. The purpose of this paper is to present an assessment of the accuracy of the dose calculations. Sensitivity calculations were used to evaluate some approximations. Then, calculated predictions were compared directly with dose measurements made with an ionization chamber (IC) in the spent-fuel coincidence counter.[1]

CALCULATIONAL METHOD

The first step of the two-step method used at Argonne National Laboratory (ANL) is computation of the gamma source in the particular assembly. A generic BN-350 reactor loading and nominal power operation cycle were modeled by Grimm and Hill at ANL using nodal transport theory, hexagonal-Z geometry, and 25-group neutron cross sections. The multigroup flux and the burnup-dependent concentrations of major actinides throughout the reactor were determined with this model. However, the model did not include explicitly the specific fission products and activation products associated with the gamma source. Rather, the solution was used to determine the axial shape of the source and to generate effective one-group cross sections and one-group flux for each radial fuel zone and each axial level. The magnitude of the fission product gamma source at the time of the measurement was found by using these cross sections and fluxes in calculations with the ORIGEN point depletion code. The specific irradiation/decay cycle history of the assembly was modeled with ORIGEN, scaling the flux magnitude in accordance with the reactor power history. The only other significant source of gammas is ^{60}Co. It was determined in basically the same way, but a fine-energy group reactor calculation was used by Hill to predict accurately the production of ^{60}Co from the stainless steel impurity ^{59}Co.

The second half of the process is a gamma transport calculation. The MCNP 4B Monte Carlo code was used to track gammas from inside the assembly to the detector surface. This is essentially a shielding calculation since there is ~7 cm of lead between the assembly and the IC. Lestone at Los Alamos National Laboratory (LANL) provided a description of the counter and how it is used. The gamma flux at the detector surface was

converted to dose rate using ANSI Standard 6.1.1 (1991) for frontal exposure.

RESULTS

Among the observations from a half-dozen calculational checks were the following:

1. Assembly burnup predictions from the approximate method described earlier were compared with predictions made by the BN-350 facility based on modeling every reactor loading and power cycle explicitly. The average error for several hundred assemblies is an 8% underprediction, and the standard deviation of the error distribution is 8%.

2. The self-protection dose is insensitive to fission product gamma spectrum approximations, but because of the energy-dependent attenuation by the lead, the IC dose is very sensitive.

3. Alternative flux-to-dose conversions change the predicted IC dose by ~20%.

High-energy-resolution gamma measurements[2] on one driver assembly were used to test an assumption related to the ^{60}Co source, namely, that the cobalt impurity concentration in the steel is 200 ppm. Staples at LANL and Blynski at BN-350 provided detailed measurement data. By comparing a computed and measured gamma intensity ratio, a ^{137}Cs (fission product) gamma line to a ^{60}Co gamma line, it was inferred that the assumed concentration is a factor of ~2 too high, at least for this assembly. Because fission product gammas dominate the IC signal, this concentration error has only an ~5% effect on the signal.

The IC dose response was calculated explicitly for four different drivers. The results, which cover a wide range of dose rates and burnups, are shown in Table I. The calculations underpredict the dose by 24 to 44%. However, when the dose is adjusted for the difference between the burnup predicted with the generic reactor model and the facility's declared burnup, the dose error is smaller and in a much narrower range.

More approximate IC dose calculations were made with a larger sample of drivers, the 45 drivers with the highest measured doses, to assess whether the dose errors in Table I are representative. The self-protection dose (in air 1 m from the driver at the axial midplane) for all drivers had been computed previously for another purpose. The new approximation was to avoid 45 gamma transport calculations by converting the self-protection dose to the IC dose using the average of conversion factors computed for the four drivers in Table I. The mean error for the resulting 45 IC dose predictions was 0.73 when no burnup adjustment was used and only slightly higher, 0.75, with the adjustment. The standard deviation of the error distribution is 0.07 with no adjustment and 0.06 with it.

TABLE I

Comparison of Calculated and Measured Doses for Four BN-350 Drivers

Case	Calculated Burnup (%)	Calculated Dose		Calculated/Measured Dose	
		Total (normalized)	% from Co	No Adjustment	Burnup Adjusted
A	3.3	1.00	7	0.76	0.82
B	3.0	0.51	11	0.56	0.73
C	4.3	1.14	8	0.58	0.71
D	9.1	3.12	10	0.76	0.78

CONCLUSIONS

The main conclusion is that the dose calculation method is reasonably accurate. Considering that the attenuation factor due to the lead in the counting system is a factor of ~400, an error of ≈25% is not large. The errors of ≈40% for two of the drivers result from unusually large mispredictions of the burnup, and even errors this large are acceptable for the applications of the dose calculations. The high sensitivity to some factors that the lead shielding creates suggests that self-protection dose predictions are probably more accurate than the IC dose predictions.

1. J. P. LESTONE et al., "The Passive Nondestructive Assay of the Plutonium Content of Spent Fuel Assemblies from the BN-350 Fast Breeder Reactor in the City of Aktau, Kazakhstan," LA-UR-00-1048, Los Alamos National Lab. (2000).

2. P. STAPLES et al., "Analysis of Gamma-Ray Spectra Obtained from Fast-Breeder Spent Nuclear Fuel," LA-UR-99-4865, Los Alamos National Lab. (1999).

6. Radiation Effects on the Microstructure and Chemical Properties of Zeolite-Y, *B. X. Gu, L. M. Wang, R. C. Ewing (Univ of Michigan)*

INTRODUCTION

Zeolites are important materials in nuclear waste management because of their applications as waste processing media, waste form, and potential backfill material in nuclear waste repositories. Rare earths, actinides, Cs, and Sr can be incorporated into the zeolites through ion exchange, which may retain and/or retard the release of radionuclides from a waste repository. Once the nuclear waste is incorporated into a final form, the ionizing radiation dose resulted primarily from β-decay can reach 10^{10} Gy after 100 yr of emplacement. Alpha-decay dose will reach values as high as 10^{18} alpha-decay events/g in periods as short as 1000 yr. This dose is well within the range for which important chemical (e.g., increased leach rate, changes in ion exchange and retention capacity) and physical (e.g., volume expansion or contraction) changes may occur in crystalline ceramics.[1–4] The objective of this work is to evaluate the long-term radiation effects on the crystalline structure and the chemical properties of zeolite using accelerated laboratory experiments with energetic H^+ beam irradiation.

MATERIALS AND EXPERIMENTAL TECHNIQUES

The material studied in this work is zeolite-NaY ($NaAlSi_2O_6 \cdot xH_2O$). Samples were irradiated with 0.5 MeV H^+ ions to the total doses of 2×10^{17}, 4×10^{17}, and 6×10^{17} ions/cm^2, respectively. The microstructure of the irradiated samples was characterized using transmission electron microscopy (TEM) and scanning electron microscopy. The ion exchange and desorption rate of the irradiated samples were measured across the sample cross section using electron microprobe analysis. The chemical bond structure in the irradiated zeolite was determined using X-ray photoelectron spectroscopy (XPS).

RESULTS

Cross-sectional TEM observation has shown that Zeolite-NaY suffers severe structural damage under proton irradiation. The crystalline-to-amorphous transition occurs at a total dose equivalent to an ionizing energy deposition of 3×10^{10} Gy and a displacement dose of 0.01 dpa. The critical amorphization dose was determined by comparing the TEM data taken from various depths with the doses calculated for the corresponding location using the computer simulation code SRIM 2000.

The ion exchange capacity of the irradiated zeolite-NaY with 10 mN CsCl solution varies with the extent of the damage to the crystalline structure. After 25 h of exchange, the Cs concentration in the amorphous region is ~0.8 wt%, which is much lower than in the undamaged region (~20 wt%). This result confirms that radiation-induced amorphization can cause a significant loss of ion exchange capacity. The results also suggest that the radiation damage by proton irradiation in zeolite-NaY is dominated by ionizing mechanism.

The release of radionuclides (Sr) from irradiated zeolite-NaSrY, after 0.5-MeV proton irradiation followed by desorption in $CaCl_2$ solution, was found to be significantly reduced as a result of radiation damage to the crystalline structure. The maximum Sr concentration was reached at the depth of 8 μm, which corresponds to an ionizing radiation dose of 2×10^{10} Gy and a displacement damage of 0.05 dpa.

One possible explanation for the reduction in ion exchange capacity and radionuclide release of the radiation-damaged zeolite is associated with the collapse of supercage, which makes the cations inside the cages inaccessible. There are three different types of cages in the zeolite-Y structure: supercages with a free aperture of 0.77 nm, sodalite cages (or β cage), and double 6-ring prisms with openings of 0.22 nm. Exchangeable cations are located in all three types of cages, with approximately two-thirds of the exchangeable cation sites located in supercages. It has been observed that the amorphization of zeolite is usually accompanied by distortion and shrinkage of the crystal. As suggested by Acosta et al.,[5] the amorphization of zeolite under electron beam irradiation is initiated from localized sites, such as the apertures of the channels. The relative sizes of the ions in solution and the apertures in the crystalline structure determine whether the ion exchange or desorption reaction will proceed. For Cs and Sr exchange, the reaction can only occur in the supercage for which the aperture size is larger than the cation size. When the crystalline structure collapses, the aperture shrinks, and exchangeable cations are trapped inside the structure. According to XPS study, radiation can cause the splitting of O 1s peak. An extra peak appears at lower binding energy, ~3 eV apart from the original O 1s peak. With the increase of radiation dose, the relative intensity of the lower energy peak increases, while the original O 1s peak decreases. In the fully amorphized sample surface, the original O 1s disappeared completely. The shift of the O 1s peak to lower binding energy upon radiation suggests a shorter atomic distance resulted from the collapse of framework structure.

CONCLUSIONS

Zeolite-Y is susceptible to radiation-induced structural damage. The damage may result in a reduction in the ion exchange capacity in the irradiated zeolite. On the other hand, radiation damage to the waste form may be beneficial. The release of incorporated radionuclides may be significantly reduced upon radiation-induced amorphization in zeolite. The collapse of channel apertures in the framework of zeolite structure is proposed as the possible mechanism for the changes in the chemical properties.

1. L. M. WANG, S. X. WANG, W. L. GONG, R. C. EWING, W. J. WEBER, *Mater. Sci. Eng.*, **A235**, 106 (1998).

2. B. X. GU, L. M.WANG, S. X. WANG, D. G. ZHAO, V. H. ROTBERG, R. C. EWING, *J. Mater. Chem.*, **10**, 2610 (2000).

3. S. X. WANG, L. M. WANG, R. C. EWING, *J. Nucl. Mater.*, **278**, 233 (2000).

4. L. M. WANG, S. X. WANG, W. L. GONG, R. C. EWING, *Nucl. Instrum. Methods*, **B141**, 508 (1998).

5. D. R. ACOSTA, G. VAZQUEZ-POLO, R. GARCIA, V. M. CASTANO, *Rad. Eff. and Def. Solids*, **127**, 37 (1993).

7. Thorium Nitrate Stockpile Stewardship and Disposition Technical Basis, *William Howard Hermes, Catherine Helen Mattus, Guillermo D. Del Cul, James W. Terry (ORNL)*

INTRODUCTION

Oak Ridge National Laboratory (ORNL) is performing work for the Defense Logistics Agency (DLA) of the U.S. Department of Defense (DOD) to assist in a future determination of the disposition for thorium nitrate hydrate $[Th(NO_3)_4 \cdot 5H_2O]$ currently stored at Hammond, Indiana, and Curtis Bay, Maryland. The DLA has ~3500 tons of ThN contained in 21 000 drums of various configurations. This material has been declared surplus to the needs of the DOD. The ORNL efforts will supply technical input to quantify the potential for use in a thorium fuel cycle and identify characterization requirements and processing requirements consistent with available waste disposition pathways.

DESCRIPTION OF THE WORK

The Defense National Support Command stores ~7 million pounds of thorium nitrate crystals (hydrate form) at two depot locations in the United States (75 wt% at the Curtis Bay, Maryland, depot and 25 wt% at the Hammond, Indiana, depot). The managing agency is the DLA. An upgrade evaluation is required to define and control risks and costs associated with long-term management of the thorium nitrate stockpile. Technical studies are underway to determine the most viable options to be compared against continued storage in the present conditions. The generalized alternatives for technical analysis include the following:

A. Retain the stockpile in the thorium nitrate form for disposal.

B. Retain the stockpile in the thorium nitrate form for long-term storage.

C. Process the stockpile to reduce the thorium nitrate to a suitable thorium form for disposal, without preserving chemical purity.

D. Process the stockpile to reduce the thorium nitrate to pure thorium oxide for long-term storage.

RESULTS

The technical assessment of option results is the focus of this paper. The methodology for analytical characterization is included because strategies are impacted by whether or not the ThN falls into a hazardous waste category. Baseline location and other relevant information are presented, as impact options, from discussions and site visits to the Nevada Test Site, uranium milling industry, rare earth processing industry, and uranium fuel production industry. An overview of option cost and scheduling methods is presented, including the baseline process flow sheet. The results from this work focus on the identification and supporting analysis of the most practical stockpile management options.

Investigation and assessment of these pathway alternatives allow for reasonable options to be identified and then analyzed in terms of technical feasibility, risk, and economics. A strategic plan will evolve consistent with the overall end states for preserving the stockpile for commercial use or phased waste disposal. Cost for stewardship must be weighed against the liabilities for continued depot storage of a material that is considered as surplus. Technical viability and order-of-magnitude economies are assessed for processing the material if a reduced form is required for the waste path.

Estimating the emissions and resource requirements for selected options in alternatives A through D is important to support follow-on programmatic efforts (i.e., the NEPA documents). Quan-

TABLE I

Life-Cycle Analysis Options (Example)

#	Option	Hammond, IN	Curtis Bay, MD	Commercial processing	Federal storage or disposal site	Commercial storage or disposal site	Life-cycle Cost $	Waste Quantity
Alt. A Option 1	Ship ThN directly to a processor; stabilize the ThN; and ship to federal disposal facility	Repack as needed to meet DOT regs and ship the ThN to processor	Repack as needed to meet DOT regs and ship the ThN to processor	Receive ThN from storage sites; stabilize the ThN; package; ship stabilized ThN to federal disposal facility	Receive and dispose of stabilized ThN	NA		
Alt. A Option 4	Ship ThN directly to commercial facility for processing and disposal	Repack as needed to meet DOT regs and ship the ThN to commercial facility	Repack as needed to meet DOT regs and ship the ThN to commercial facility	NA	NA	Receive, process, and dispose of Th in final form		
Alt. A Option 5	Ship ThN directly to commercial uranium mill for processing and disposal	Repack as needed to meet DOT regs and ship the ThN to commercial uranium mill	Repack as needed to meet DOT regs and ship the ThN to commercial uranium mill	Receive, process to recover source material, and retain process wastes on the site	NA	Retain process wastes in an onsite 11e(2) disposal facility		
Alt. B Option 6	**BASELINE** Upgrade packaging as required for transport	Leave the ThN at Hammond; upgrade packaging as needed to meet DOT regs and preserve container integrity	Leave the ThN at Curtis Bay; upgrade packaging as needed to meet DOT regs and preserve container integrity	NA	NA	NA		

TABLE II

Pathways for the Thorium Nitrate Project with Qualitative Ratings (Example)

#	Option	Hammond, IN	Curtis Bay, MD	Commercial processing	Federal storage or disposal site	Commercial storage or disposal site	Criteria[a]					Status
							Life cycle cost, $	Waste quantity	Health & safety impacts	Environmental impacts	Programmatic risk/impacts	
Alternative A–Retain in the thorium nitrate form for disposal												
1	Ship ThN directly to a processor; stabilize the ThN; and ship to federal disposal facility	Repack as needed to meet DOT regs and ship the ThN to processor	Repack as needed to meet DOT regs and ship the ThN to processor	Receive ThN from storage sites; stabilize the ThN; package; ship stabilized ThN to federal disposal facility	Receive and dispose of stabilized ThN	NA	TBD	TBD	SD	N	SI	Medium
2	Ship ThN to Curtis Bay; ship ThN to commercial facility for processing and disposal	Repack as needed to meet DOT regs and ship the ThN to Curtis Bay	Repack as needed to meet DOT regs; receive ThN from Hammond; and ship the ThN to commercial disposal site	NA	NA	Receive, process, and dispose of Th in thorium nitrate final form	TBD	TBD	SD	N	SD	Low

titative means will be used wherever feasible to measure risk and costs to provide decision makers the best information to narrow the future program purpose and need to the most reasonable alternatives.

In alternative C, the thorium nitrate stockpile would be converted to an end state in order to meet criteria for acceptance at a disposal site. In alternative D, the thorium nitrate stockpile would be converted to a reduced form for long-term storage and potential use in the thorium fuel cycle. Examples of feasible options (more than 35 options defined for sponsor consideration) to be used for detailed transport, risk, and cost analysis are defined in Table I.

An extensive list of pathways for the thorium nitrate stockpile was established. Each pathway is named, and the associated action at the Curtis Bay and Hammond depots is described. As appropriate, follow-on actions at an off-site location are described. The off-site action may be processing, storage, or disposal.

Each pathway (option) is evaluated on five criteria that were selected to be representative of guidelines typically used by federal decision makers. Three criteria were evaluated qualitatively, and the remaining two are used for quantitative measures that will be developed as part of the project. The criteria are summed to reach the value given in the status column.

The acronyms used in this analysis are MD = major decline; MI = major improvement; NC = no change; NA = not applicable; SD = some decline; SI = some improvement; and TBD = to be determined. An example of results reporting is provided as Table II.